A Marie-Curie-ITN within H2020

migrate microfluidics

ISTEGIM 2019

Proceedings of the International Symposium on Thermal Effects in Gas flows In Microscale October 24-25, 2019 – Ettlingen, Germany

istegim2019:283998

A HYBRID NUMERICAL METHODOLOGY BASED ON CFD AND POROUS MEDIUM FOR THERMAL PERFORMANCE EVALUATION OF A DOUBLE LAYER GAS-TO-GAS MICRO HEAT EXCHANGER IN COCURRENT AND COUNTERFLOW CONFIGURATIONS

Danish Rehman*[1], Joseph Jojomon[2,3], GianLuca Morini[1], Michel Delanaye[2], and Jurgen Brandner[3]

[1]**Microfluidics Lab., University of Bologna, Via del Lazzaretto 15/5, 40131 Bologna, Italy**
[2]**MITIS SA, Rue Bois Saint-Jean, 3 4102 Seraing, Belgium**
[3]**Institute of Microstructure Technology (IMT), Karlsruhe Institute of Technology, D-76344 Eggenstein-Leopoldshafen, Germany**

Abstract

In micro heat exchangers, due to the presence of distributing and collecting manifolds as well as hundreds of parallel microchannels, a complete conjugate heat transfer analysis requires a large amount of computational power. Therefore in this study, a novel methodology is developed to model the microchannels as porous medium where a compressible gas is used as working fluid. With the help of such reduced model, a detailed flow analysis through individual microchannels can be avoided by studying the device as a whole at considerably less computational cost. A micro heat exchanger with 133 parallel microchannels (average hydraulic diameter of 200 μm) in both cocurrent and counterflow configurations is investigated in the current study. Hot and cold streams are separated by a stainless-steel partition foil having thickness of 100 μm. Rectangular microchannels have a cross section of 200 $\mu m \times 200$ μm with wall thickness of 100 μm in between. As a first step, a numerical study for conjugate heat transfer analysis of microchannels only, without distributing and collecting manifolds is performed. Mass flow inside hot and cold fluid domains is increased such that inlet Reynolds number for both domains remains within the laminar regime. Inertial and viscous coefficients extracted from this study are then utilized to model pressure and temperature trends within porous medium model. In order to cater for density dependence of inertial and viscous coefficients due to compressible nature of gas flow in microchannels, a modified formulation of Darcy-Forchheimer law is adopted. A complete model of a double layer micro heat exchanger with collecting and distributing manifolds where microchannels are modeled as porous medium is finally developed and used to estimate the overall heat exchanger effectiveness of the investigated micro heat exchanger. A comparison of computational results using proposed hybrid methodology with previously published experimental results of the same micro heat exchanger showed that adopted methodology can predict the heat exchanger effectiveness within the experimental uncertainty for both cocurrent and counterflow configuratons.

KEYWORDS: Reduced model, LMTD method, CHT, compressible fluid

1. INTRODUCTION

Originally proposed for estimating pressure drop of incompressible flow over bed of spheres, Darcy's Law has been extended to multiple parallel microchannels (MCs) in heat sinks. An analytical model was first developed by Kim et al. [1, 2] where they modeled the MCs as porous media and compared modeling results with experimental results of Tuckerman & Pease [3] as well as with Knight et al. [4]. Results showed that developed model can be used for thermal performance and optimization of MC heat sinks. The same model has been studied by

*corresponding author: danish.rehman2@unibo.it

Liu and Garimella [5] and improved by Lim et al. [6]. Porous media based analytical models tend to solve a three equations model for fluid flow and heat transfer through MC heat sinks using simplified momentum and energy equations. A common trait of all the studies conducted for MC heat sinks is the use of an incompressible fluid. A porous medium approximation of a compact heat exchanger used in micro gas turbine application has recently been presented by Joseph et al. [7, 8]. Channel dimensions and operating pressure were such that gas was incompressible whereas operating temperature of the hot fluid was higher than $1000\ K$. A porous model approximation for a double layered micro heat exchanger (μHx) where gas undergoes strong compressibility, has recently been presented by the authors [9], for parallel flow arrangement. In current study the previously reported work is extended to cover the counterflow arrangement as well and detailed comparisons between experimental and numerical results for both flow configurations are being presented.

In this work a two step methodology is proposed to conduct a performance evaluation study on μHx with acceptable computational power. As a first step, a $3D$ conjugate heat transfer (CHT) model of gas to gas μHx is developed without distributing and collecting manifolds. Resulting pressure, velocity and temperature fields are utilized to calculate inertial and viscous coefficients of the modified Darcy's porous law. A complete single layer of μHx with manifolds is then modeled with boundary conditions such that MCs are modeled as a porous medium with a low resolution mesh. This is achieved by modeling the required pressure drop as a momentum source term using inertial and viscous coefficients of porous medium and applying a free slip boundary condition at all MC walls. Similarly to incorporate heat transfer in MCs core, a source term derived by CHT analysis of MCs only, is also introduced in the complete single layer model.

2. BACKGROUND

Pressure drop (Δp) of a fluid through a porous medium of length L can be expressed using an extended Darcy-Forchheimer (here after referred to as simply Darcy) law as follows:

$$\frac{-\Delta p}{L} = \frac{\mu \dot{G}}{\alpha \rho} + \frac{\Gamma \dot{G}^2}{2\rho} \tag{1}$$

where $\frac{1}{\alpha}$ is viscous coefficient representing porous medium permeability and Γ is an inertial coefficient of the Darcy's law, ρ and μ denote density and dynamic viscosity of the fluid respectively, and $\dot{G}$ denotes mass flow rate ($\dot{m}$) per unit area A ($\dot{G} = \dot{m}/A$). Calculation of viscous ($\frac{1}{\alpha}$) and inertial (Γ) coefficients, is usually done using experimental pressure drop results and therefore various empirical relations exist for different porous media geometries. No such experimental relations exist for the gas flows in μHx, however. As mentioned earlier, in this work porous medium coefficients are extracted from CHT analysis using a modified Darcy law. Thus integrating Eq.(1) in the streamwise direction 'x' of the MC yields:

$$\int_{in}^{out} \frac{-\Delta p}{L} dx = \frac{\mu \dot{G}}{\alpha} \int_{in}^{out} \frac{dx}{\rho} + \frac{\Gamma \dot{G}^2}{2} \int_{in}^{out} \frac{dx}{\rho} \tag{2}$$

Combining gas law and a first order Taylor approximation of temperature change along the length of the MC, and then integrating the resulting equation between inlet 'in' and outlet 'out' of the MC after performing some mathematical manipulations on Eq.(2), it yields:

$$\frac{-\Delta p}{L} = \mu \xi \dot{G} \left(\frac{1}{\alpha}\right) + \frac{\xi \dot{G}^2}{2} (\Gamma) \tag{3}$$

where $\xi = \frac{1}{\ln\left(\frac{\rho_{out}}{\rho_{in}}\right)} \left(\frac{1}{\rho_{in}} - \frac{1}{\rho_{out}}\right)$. Boundary conditions of CHT analysis are chosen such that there are no heat losses to the surroundings, therefore all the heat loss by hot fluid must be shared between partition foil (solid wall) and cold fluid. Therefore porous medium coefficients can be extracted from either side of the CHT

model. In this work, inertial and viscous coefficients are extracted from the channel with hot fluid. From a CHT analysis of MCs only, all parameters in the Eq.(3) are available for a specific mass flow, with inertial and viscous coefficients as the only two unknowns. However, if Eq.(3) is applied to two consecutive mass flows $\dot{m}_i$ and $\dot{m}_{i+1}$, an average value of both the coefficients between these mass flows can be found out by solving a system of two linear equations for two unknowns. This is repeated for range of mass flows being studied and a polynomial fit on these evaluated coefficients is used as an input for the porous model. Similarly a volumetric heat loss of hot fluid channel is calculated for all mass flows from CHT analysis using $\dot{q_v} = \frac{\dot{m}C_p\Delta T}{AL}$, where C_p is the specific heat of fluid at constant pressure. A polynomial fit onto this volumetric heat loss is given as a source term in energy equation while solving for porous model.

3. NUMERICAL METHODOLOGY

As described earlier, two different numerical setups are used in the current work. First a $3D$ CHT of MCs only, without distributing and collecting manifolds is performed. Secondly, using the results from CHT model, performance of complete heat exchanger with manifolds is analyzed. Reynolds number at the inlet of MC is defined by:

$$Re = \frac{\dot{m}D_h}{\mu A} \tag{4}$$

where hydraulic diameter (D_h) of a rectangular MC with width (w) and height (h) is defined as:

$$D_h = \frac{2wh}{w+h} \tag{5}$$

From CHT analysis, heat transfer rate ($\dot{Q}$) on hot (h) and cold (c) side can be defined by using respective flow quantities as:

$$\dot{Q} = \dot{m}C_p\Delta T \tag{6}$$

Overall heat transfer coefficient is calculated by:

$$U = \frac{\dot{Q}_{av}}{A\Delta T} \tag{7}$$

where $\dot{Q}_{av} = \frac{\dot{Q}_c+\dot{Q}_h}{2}$, is the average value of the heat transfer evaluated on the cold and hot side of μHx. Finally heat exchanger effectiveness, defined as the ratio of actual heat transfer rate and maximum potential heat transfer rate available, can be calculated using:

$$\varepsilon = \frac{Q_{av}}{(\dot{m}C_p)_{min}(T_{h,in} - T_{c,in})} \tag{8}$$

For porous model of μHx, heat exchanger effectiveness to be compared with experimental results, is calculated for the MC core only. This essentially means that temperature difference from the inlet of MC core to outlet of MC core is used to calculate ε. Moreover, as only one layer is computationally modeled in porous model, resulting effectiveness is calculated as follows:

$$\varepsilon_p = \frac{Q_p}{(\dot{m}C_p)_p(T_{h,in} - T_{c,in})} = \frac{\overline{T}_{MC,in} - \overline{T}_{MC,out}}{T_{h,in} - T_{c,in}} \tag{9}$$

where subscript 'p' denotes the porous model. $\overline{T}_{MC,in}$ and $\overline{T}_{MC,out}$ denote the mass flow weighted averages of static temperatures, at the inlet and outlet of N number of MCs, respectively. In order to extract inertial and viscous coefficients for the porous medium using methodology outlined earlier, a $3D$ CHT model is setup where only MCs are modeled without considering both collecting and distributing manifolds. However, to allow any

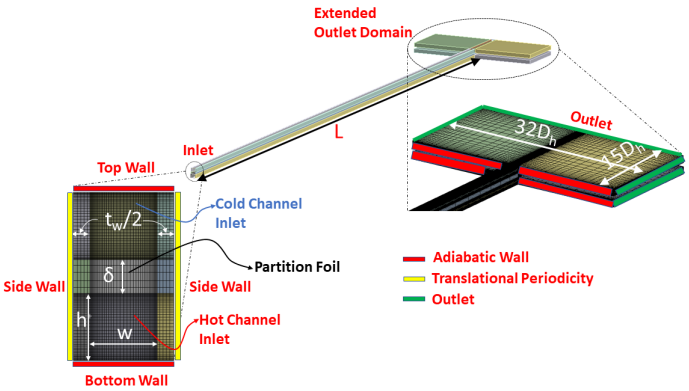

Figure 1: Mesh and geometric details for co-current CHT analysis

possible underexpansion at the outlet of hot and cold MCs, computational domain is extended $15D_h$ in the streamwise and $32D_h$ in the lateral direction as shown in Fig. 1. A meshed model for a complete layer of μHx is also shown in Fig. 2. Geometry and meshing for both models are done using Design Modeler and ANSYS Meshing software respectively. A mesh of $40 \times 40 \times 100$ is used in the MCs for CHT analysis whereas a coarse mesh of $3 \times 3 \times 40$ is used for MCs in case of porous model. Mesh is refined near the walls to capture any flow vortices present in the model. A commercial solver CFX based on finite volume methods is used for the flow simulations. Ideal Nitrogen gas is used as working fluid for both models. Simulation relevant parameters used in analyses are tabulated in Table 1. Laminar flow solver is used for CHT model whereas a transient turbulence

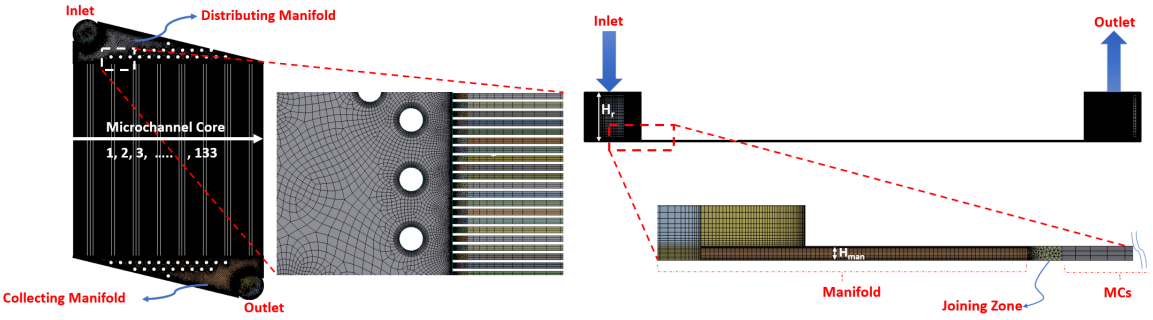

(a) (b)

Figure 2: Geometry and mesh details of porous model: top view **(a)**, and side view **(b)**

Table 1: μHx geometry used for simulations.

Parameter	**Symbol (units)**	**Value**
MC width	$w\ (\mu m)$	200
MC height	$h\ (\mu m)$	200
MC Length	$L\ (\mu m)$	40
Hydraulic Diameter	$D_h\ (\mu m)$	200
Wall Thickness	$t_w\ (\mu m)$	100
MC housing (PMMA) conductivity	$k_{MC}\ (W/m/K)$	0.25
Partition Foil (Stainless Steel) thickness	$\delta\ (\mu m)$	100
Partition Foil conductivity	$k_{PF}\ (W/m/K)$	15

model $\gamma - Re_\theta$ [10, 11] is utilized for porous model. Higher order advection scheme available in CFX is utilized and pseudo time marching is done using a physical timestep of 0.01s. A convergence criteria of 10^{-6} for RMS residuals of governing equations is chosen while monitor points for pressure and velocity at the MC inlet and outlet are also observed during successive iterations. In case where residuals stayed higher than supplied criteria, the solution is deemed converged if monitor points did not show any variation for 200 consecutive iterations. Reference pressure of $101kPa$ was used for the simulation and all the other pressures are defined with respect to this reference pressure. Energy equation was activated using Total energy option available in CFX which adopts energy equation without any simplifications in governing equations solution. Kinematic viscosity dependence on gas temperature is defined using Sutherland's law. Further details of boundary conditions used in CHT and Porous model can be found in Tables 2 and 3 respectively. Using CHT model, global as well as local evolution

Table 2: Boundary conditions used in the CHT Analysis.

Boundary	**Value**	
	Hot Side	**Cold Side**
Inlet	- $\dot{m}$ evaluated using Eq. 4 for cold side - $T_{h,in} = 90$ °C	- $T_{c,in} = 20$ °C
Side Walls	Translational Periodicity	
Top & Bottom Walls	Adiabatic	
Outlet	Pressure outlet, Relative p = 0 Pa	

Table 3: Boundary conditions used in the porous model for μHx.

Boundary	**Value**
Inlet	- $\dot{m}$ from experimental testing - $T_{h,in} = 90°C$
MCs walls	Free slip
Inertial and visocus coefficients	Determined from CHT analysis
Energy source term	Determined from CHT analysis
Manifolds walls	Adiabatic/ No slip
Outlet	Pressure outlet, Relative p = 0 Pa

of flow variables with inlet mass flow is evaluated at six different cross-sectional planes defined at x/L of 0.005, 0.1, 0.5, 0.9, 0.95 and 0.995 respectively. In addition, two planes defined at x/L of 0.0001 and 0.9995 are treated as the inlet and outlet of MC, respectively. Results from these planes for both hot and cold fluid sides are further post processed in MATLAB to deduce required flow quantities. Thermal effectiveness is then simply evaluated using Eq. 8. Once the porous medium coefficients namely inertial (Γ) and viscous ($\frac{1}{\alpha}$) are determined using CHT model of a double layer μHx, next step is to setup a complete single layer porous model with inlet and outlet manifolds. A gas to gas double layer μHx that has been experimentally investigated previously by Yang et al. [12, 13] and Gerken et al. [14], is used for validation of proposed methodology.

4. RESULTS

4.1. CHT Model

CHT model with linear periodicity at side walls represents an ideal situation where there exists no maldistribution for parallel MCs. This essentially means that all parallel MCs would have same mass flow at their respective inlets and manifold does not play a significant role in the peformance evaluation. Results for the heat transfer rate for both cocurrent and counterflow configurations are shown in Fig. 3. For an incompressible fluid, heat

transfer rate using numerical model on both sides should be equal. But for gases, as the gas flow experiences additional acceleration due to compressibility, heat gain on the cold side tends to differ than heat loss on the hot side. An interesting fact is that heat transfer rate on the hot side keeps on increasing with increasing mass flow. On the contrary, it keeps on decreasing on the cold side. This holds true for both cocurrent and counterflow configurations. Therefore even though there are no losses modeled to the surroundings in the CHT model, due to compressibility effects gas flows still exhibit difference in heat transfer rate between hot and cold sides.

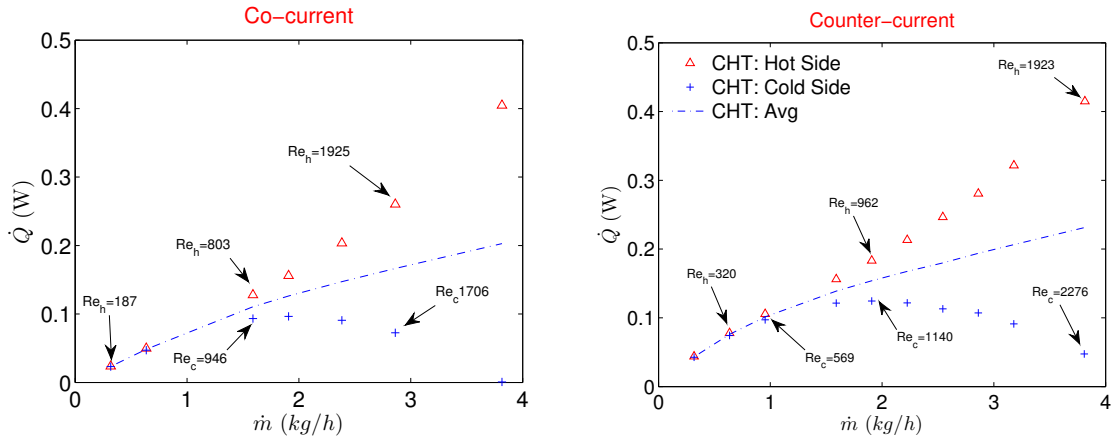

Figure 3: Heat transfer rate for CHT analysis when flow configuration is cocurrent (**a**), and counterflow (**b**).

Similar behavior can also be seen in effectiveness where it increases with mass flow for hot fluid and decreases for the cold fluid as shown in Fig. 4. This is simply because gas flow accelerates at the expense of

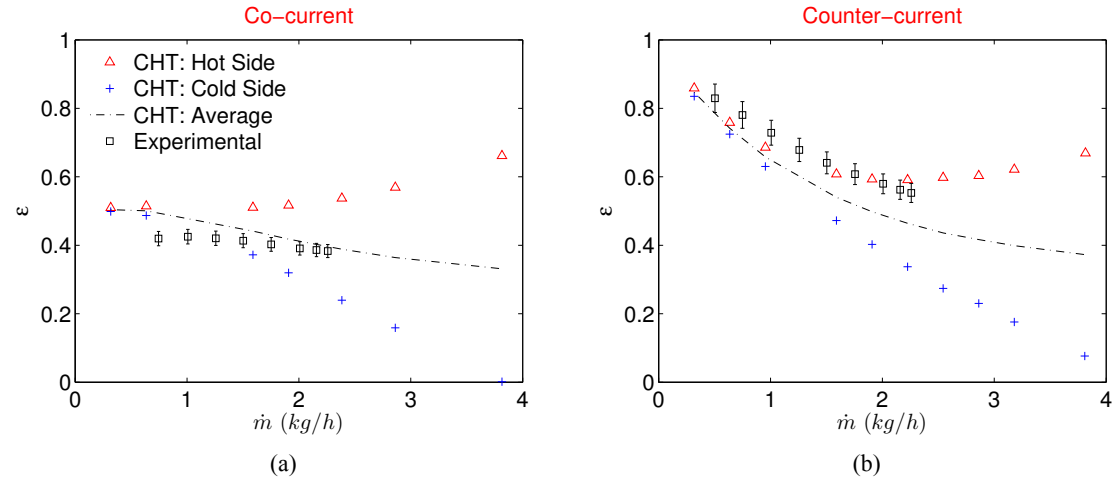

Figure 4: Heat exchanger effectiveness for CHT analysis when flow configuration is cocurrent (**a**), and counterflow (**b**).

kinetic energy, therefore a part of total energy is utilized for acceleration than to have a conjugate heat transfer. Therefore for gas to gas μHxs, it is not recommended to operate in high mass flow regimes because at higher mass flows, gas flows experience a "self cooling" phenomenon at the expense of higher pressure drop. This phenomenon is evident by Fig. 5 which shows the evolution of the temperature at the center line of both fluid streams and partition foil (solid) along the direction of the flow. For smaller mass flows (Re) temperature profiles of hot and cold streams are reminiscent of a heat transfer process between incompressible fluids for cocurrent configuration where temperature of hot and cold fluids are symmetric and partition foils assumes an

average constant temperature of the two sides. As fluid velocities increase at the inlets of respective streams, profile symmetry deteriorates with partition foil assuming a temperature that is more influenced by hot side than the cold fluid side. Outlet temperature of the hot fluid keeps on decreasing with an increased mass flow rate signaling a better heat transfer process. However, if one is to look at the outlet temperature of the cold fluid instead, it also keeps on decreasing significantly than the inlet with increasing mass flow rates. This signifies that cold fluid stream is utilizing the transferred thermal energy from the hot stream, only to increase the velocity (kinetic energy). It is well known that gas microflows, due to compressible nature accelerate at the expense of thermal energy of the fluid [15, 16, 17, 18]. Similarly a higher decrease of temperature and pressure very close to the

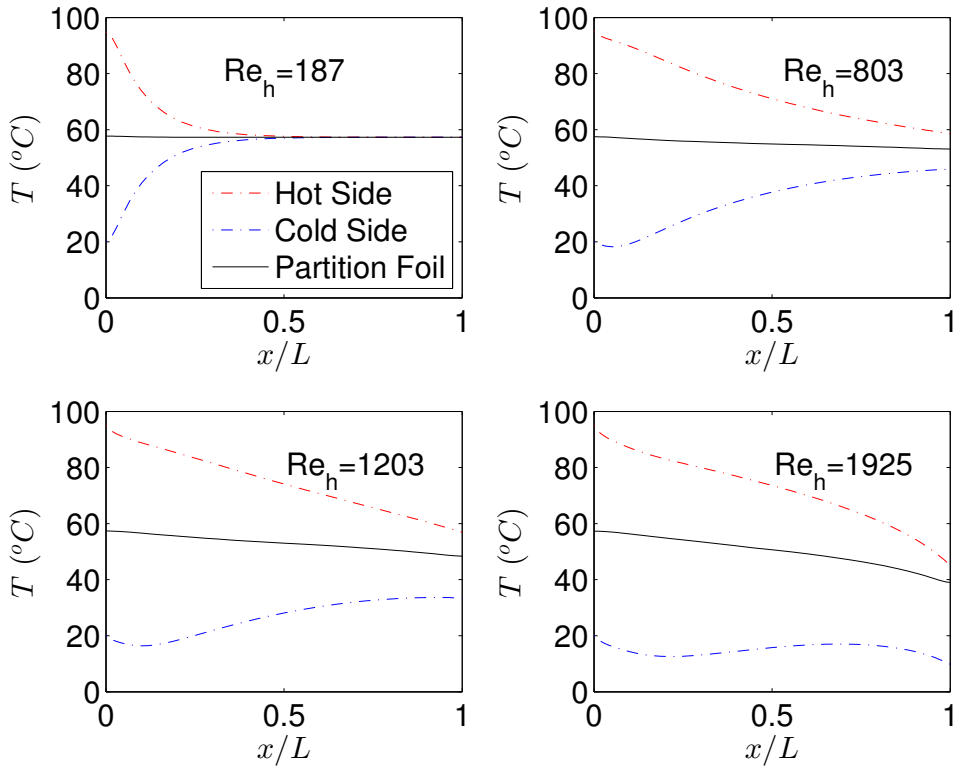

Figure 5: Temperature along the length of the hot and cold MCs for various Re in cocurrent flow configuration

outlet of the MC for hot fluid stream is also due to sudden expansion of the gas due to compressibility. In result to this strong compressibility effect, gases in both fluid streams are actually utilizing respective thermal energies and converting them in kinetic energy which is deteriorating to the overall heat transfer process. Temperature decrease of the cold stream is such that the static temperature at the outlet is lower than the inlet value showing no active participation of cold fluid stream into the overall heat exchange of the device at higher mass flow rates. This also explains the decrease of $\dot{Q}$ in Fig. 3 on the cold side of the μHx and a continuous increase of $\dot{Q}$ on the hot side with increasing mass flow rates. For data reduction of the most experimental investigations, an average value of $\dot{Q}$ is used to calculate the overall heat transfer coefficient (U) to further evaluate the heat exchanger effectiveness (ε). This is done due to practical limitation of the heat losses to the surroundings in the laboratory environment from both streams. Similar approach has been used by Yang et al. [19, 12, 13] and Koyam et al. [15, 16] for gas to gas μHxs. There are heat losses to the surroundings in a typical experimental campaign but as shown in this work, given a good insulation of the μHx, the real reason for the deviation of $\dot{Q}$ on hot and cold fluid streams in a gas to gas μHx might actually stems from gas compressibility. Therefore, numerical results of ε are calculated with an average $\dot{Q}_{ave}$ from CHT analysis and are compared with experimental results of Yang et al. [13] in Fig. 4. For a cocurrent configuration, a CHT analysis overestimates the average ε as compared

to experimental results for all the mass flows considered in this study. Difference between the two decreases though at higher mass flow rates. On the contrary ε for counterflow configuration is underestimated by CHT analysis for complete range of mass flows investigated. Such discrepancies between experimental results of μHx and an equivalent CHT analysis with periodic boundary conditions are expected as CHT model used in this study is devoid of flow maldistribution effects. Also, any temperature change that might occur in the manifolds due to flow deceleration caused by the presence of numerous circular pillars in distributing and collecting manifolds, is not catered for. Further step is to evaluate the inertial and viscous coefficients of the modified

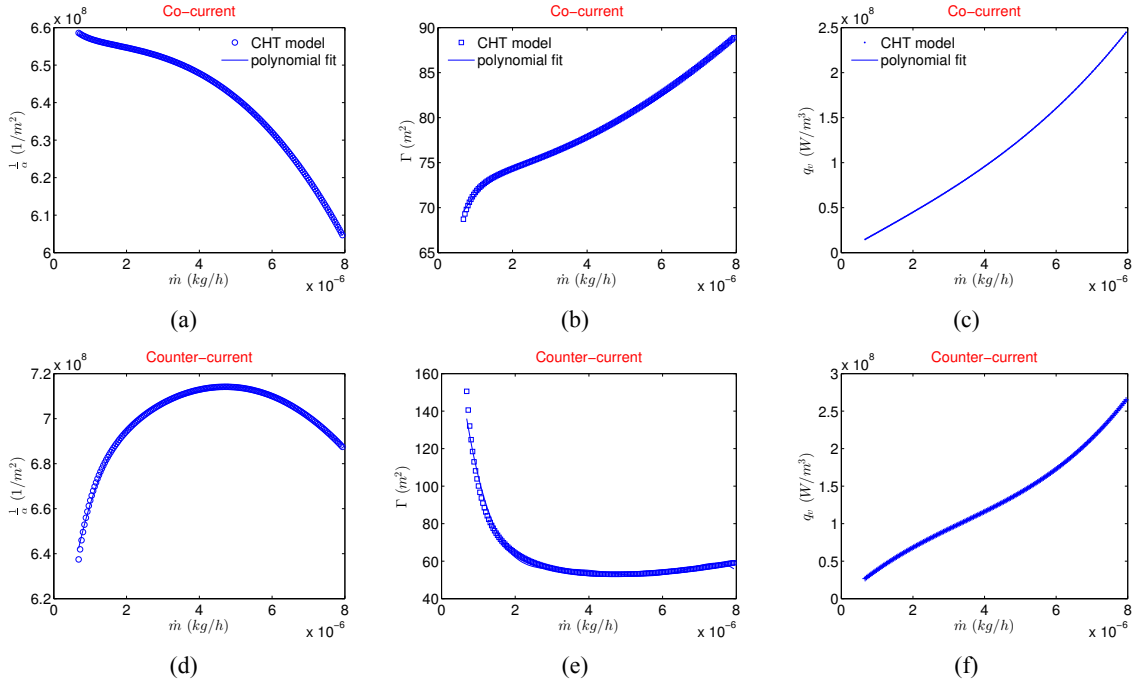

Figure 6: Viscous coefficient (**a**, **d**), inertial coefficient (**c**, **e**), and volumetric heat source term (**c**, **f**) extracted from CHT analysis in both flow configurations.

Darcy's law using flow quantities evaluated in CHT analysis. For this reason, flow characteristics are extracted at various planes along the length of the hot and cold fluid MCs. These are used to form a set of linear system of equations to solve for porous medium coefficients utilizing the methodology outlined in Section 1. Solution of these system of equations for various mass flow rates results in data points where a polynomial with mass flow rate as dependent variable can be fit to be given as input to the porous medium model available in ANSYS CFX. In theory, for the range of inlet gas temperatures considered in this study pressure drop from hot side and cold side should be almost similar and furthermore it should be independent of the flow configuration. Therefore any side of the fluid stream (hot or cold) from CHT analysis can be used to evaluate porous medium coefficients. For the scope of this work, hot fluid side is used to evaluate porous medium coefficients. Resulting viscous and inertial coefficients are shown in Fig. 6 (a, b, d, e) for both cocurrent and counterflow configurations.

To model the desired temperature drop on the hot fluid side, a source term q_v is extracted from the hot fluid stream of CHT analysis. Variation of this volumetric heat source term with the mass flow rate is shown in Fig. 6c (cocurrent) and 6f (counter flow). A polynomial fit on this q_v is given as a source term to energy equation in porous model of μHx.

4.2. Porous Model

Presence of manifolds introduces flow maldistribution that affects both pressure drop as well as heat exchanger effectiveness of a μHx compared to earlier performed CHT analysis. A single layer of the μHx as shown in Fig.

2 is considered in the porous model. This is due to the fact, that pressure and temperature drops of hot side from CHT analyses that are used to extract porous medium coefficients and source term respectively, already catered for any conjugate heat transfer effects of both layers. Therefore modeling only one layer with these coefficients and source term should be sufficient to emulate a double layer μHx. Moreover, as porous media coefficients as well as source term are mass flow rate dependent, based upon encountered maldistribution each MC will exhibit respective pressure and temperature drop along the length. Experimental pressure drop of the double layer μHx being considered in this study for different flow configurations has been reported by Gerken et al. [14]. Pressure drop showed dependence on the flow configuration as well as the material and thickness of the partition foil employed during the experimental tests. A possible reason of this deviation between different foil materials and thicknesses was associated with possible bending of the thin partition foils inside manifolds although a strong layer of circular pillars were realized underneath (in manifolds) to protect against such undesired deflection of partition foil. Computational results of pressure drop from porous model are compared with the experimental results reported for the same μHx from two different studies [13, 14] in Fig. 7. As results differ from one separation foil material to the other, only results with stainless steel foil with thickness of 100 μm (as utilized in current study) are compared and are shown in Fig. 7a. It can be seen that total pressure drop of the device

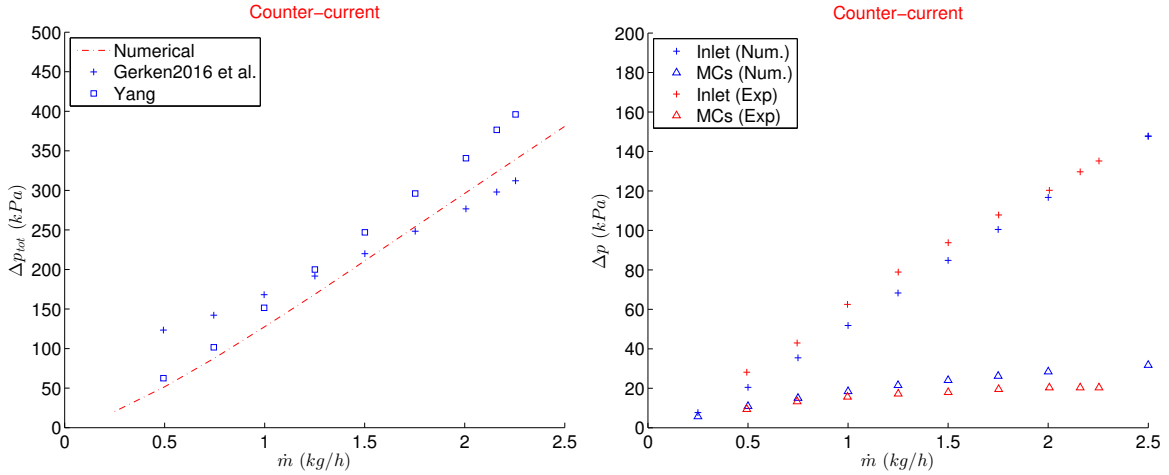

(a) (b)

Figure 7: Comparison between experimental and numerical total pressure drop of μHx **(a)**, and in the inlet and MCs only **(b)**

shows a good agreement between the average of two experimental investigations on the same μHx. Results are more compliant to the results of Yang et al. [13] for smaller mass flows while they match better with Gerken et al. [14] for higher mass flow rates. Pressure drops in the distributing manifold and MC core are also shown in Fig. 7b where there exists a very good match between current porous model and experimental results of Gerken et al. [14]. However, pressure drop of MC core is slightly overestimated at higher mass flow rates with modeled porous medium coefficients with incorporated source term in energy equation.

Flow maldistirbution is shown in Fig. 8 for both cocurrent and counterflow configurations where MC indexing is done as outlined in Fig. 2a. Contrary to the intuition, maldistribution shows dependence on the flow configuration where it is in general less for cocurrent configurations than counterflow arrangement. Due to presence of circular pillars, maldistribution does not exhibit a typical profile to be expected of triangular manifolds [20, 8]. Another reason for this could be the orthogonal direction of inlet with reference to channel flow whereas in most experimental as well as numerical studies, an inline flow is encountered where fluid enters parallel to the base plane of distributing manifold.

To compare the effect of heat transfer on the flow maldistribution, counterflow porous model results are calculated at mass flow rate of 2.5 kg/s by deactivating the energy source term and results are shown in Fig. 9.

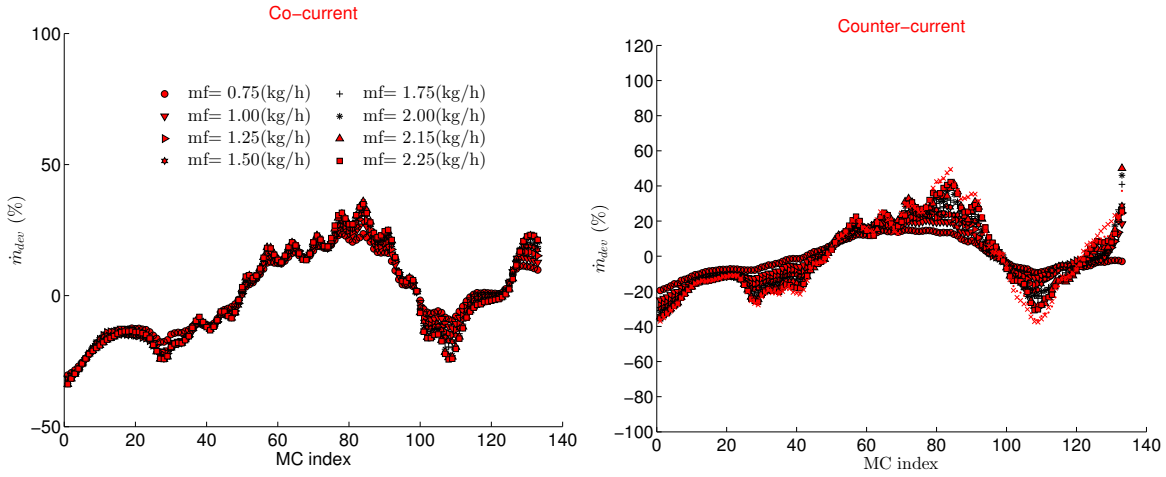

(a) (b)

Figure 8: Flow maldistribution in MCs for cocurrent flow (**a**), and counterflow (**b**).

It is evident that temperature drop does not substantially affect the maldistribution pattern in the middle core of

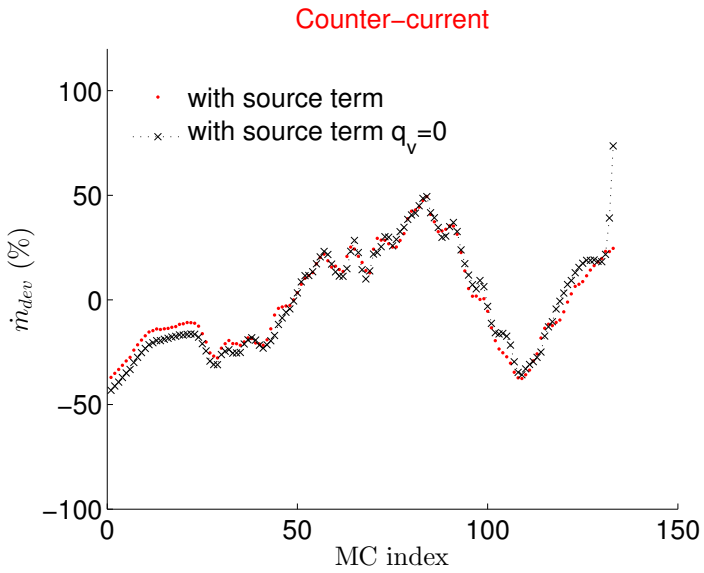

Figure 9: Flow maldistribution with (a) and without (b) source term q_v for counterflow configuration with $\dot{m}_f = 2.5\ kg/s$

the current manifold while it is higher on the either extremes for the case when source term is not modeled. In other words, for current configuration heat transfer helps decreasing the maldsitribution in first and last MCs. Heat exchanger effectiveness evaluated using Eq. 9 is shown in Fig. 10 for both flow configurations. In experimental campaign, one pressure and two temperature sensors were placed $0.4\ mm$ from the inlet and outlet of the MCs core to represent an average value of pressure drop and temperature drop or gain through hot or cold side of MCs core. For a cocurrent configuration, porous model predictions match to the experimental results within the experimental uncertainty. However for the counterflow configuration, results of porous model seem to underestimate the ε compared to experimental results. To investigate this discrepancy, average fluid temperatures at two planes of $0.5\ mm \times 0.5\ mm$ are used in the vicinity of the locations where experimental temperature sensors were placed. Average temperature of the gas is then calculated using a simple equal weighted average of these two temperatures as done in experimental campaign. Therefore, as it can be seen in Fig. 10b when

temperature estimation at the inlet and outlet of MCs core is done in a way that is close to experimental settings, it resulted in a higher temperature drop which translated into an apparent increase in ε. However when mass flow weighted averages of temperatures at inlet and outlet of MC core are considered from numerical simulations, resulting ε is slightly lower than what has been reported for experimental tests. On the other hand, limited number of sensors are practical limitation inside micro devices therefore averaging performed using a limited number of temperature and pressure sensors would always result in a slight discrepancy between experimental and numerical global characteristics of the μHxs. Results of ε from porous model are also compared with the CHT analysis. It can be noted from Fig. 10b that porous model with all the flow maldistribution results in an overall heat exchanging efficiency that is identical to that of a simple CHT model without manifolds, for the counterflow configuration. Similar conclusion was also presented by Joseph et al. [8] where CHT analysis with

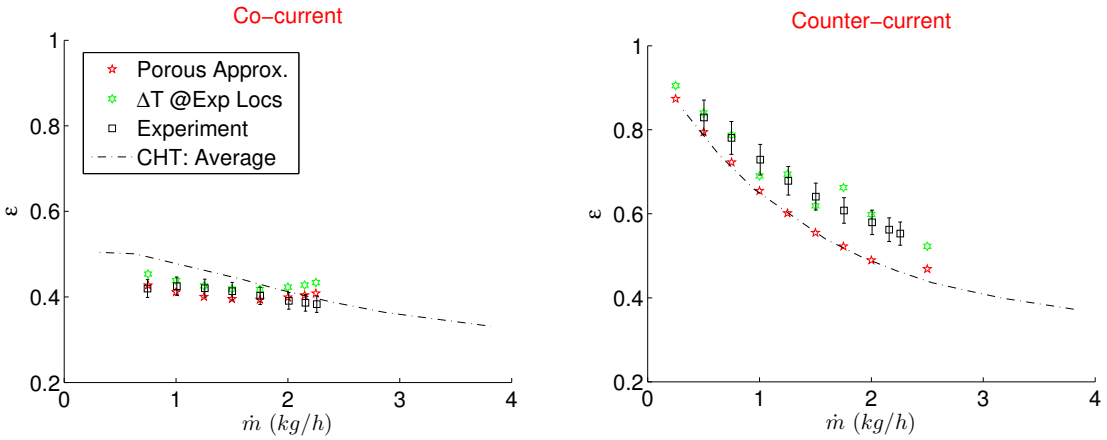

Figure 10: μHx effectiveness for cocurrent flow (**a**), and counterflow (**b**).

periodic side walls for a 60 layered counterflow compact heat exchanger showed only 4 % deviation in ε compared to experimental results. This points to the fact, it is sufficient to use a CHT model to predict the thermal effectiveness of a multilayered parallel channel counterflow μHx. Pressure drop analysis of the entire device however, cannot be performed using only CHT analysis as there is a significant pressure drop in the distributing and collecting manifolds. On the contrary, ε results for the cocurrent configuration show a dependence on the maldistribution where porous model and experimental results are different than CHT model with CHT model over estimating the ε when compared to porous model.

5. CONCLUSIONS

Independent of the flow configurations investigated in this study, the developed porous medium based numerical model shows an excellent match with experimental results for both cocurrent and counterflow configurations. Moreover, as flow inside porous MCs is not treated as wall bounded rather a free slip boundary condition is applied, a substantial amount of computational power is saved in the process. Since proposed porous medium model requires only one layer of μHx, with MCs core modeled as porous medium, it eliminates the need of simulating all the layers of such micro device where a layered structure is quite common and an effort to computationally model such device with all the layers would require a staggering amount of computational power. Therefore the proposed model for the analysis of parallel channel μHx can prove to be a feasible option for rapid design optimization in engineering studies. Based on the discussion conducted earlier, following conclusions can be inferred:

1. Overall heat exchanger effectiveness of a μHx in a counterflow configuration is identical to that of the CHT analysis on the range of mass flows investigated in this study. For a cocurrent configuration however,

heat exchanger effectiveness from porous model matches well with experimental results while CHT model overpredicts it.

2. Pressure drop of porous model is much higher compared to the CHT due to presence of collecting and dividing manifolds. Pressure drop estimation using porous model is in good agreement with the experimental results of the same μHx.

3. Porous medium coefficients for parallel channel μHx can be extracted for compressible fluids by modifying the existing Darcy-Forchheimer law to incorporate for the strong density variations with increasing mass flow rates in MCs.

4. Compared to meshing strategy adopted in CHT analysis, porous model results in saving of atleast 20 million computational nodes for the double layer gas to gas μHx investigated in this study with good enough predicitions of global pressure drop and heat exchanger effectiveness.

5. CHT analysis revealed that gas in both hot and cold fluid streams experiences a "self-cooling" phenomenon where temperature of the gases keeps on decreasing from inlet to the outlet at higher mass flow rates (Re). Therefore for a μHx operating under balanced mass flow rates, smaller values of mass flow rates are recommended.

ACKNOWLEDGEMENTS

This research received funding from the European Union's Framework Programme for Research and Innovation Horizon 2020 (2014–2020) under the Marie Sklodowska-Curie Grant Agreement No. 643095 (MIGRATE Project).

REFERENCES

[1] S. J. Kim and D. Kim, "Forced convection in microstructures for electronic equipment cooling," *ASME J. Heat Transfer*, vol. 121, no. 1-–12, pp. 639–645, 1999.

[2] S. J. Kim, D. Kim, and D. Y. Lee, "On the local thermal equilibrium in microchannel heat sinks," *Int. J. Heat Mass Transfer*, vol. 43, no. 1-–12, pp. 1735–1748, 2000.

[3] D. Tuckerman and R. Pease, "High-performance heat sinking for vlsi," *IEEE Electron Device Lett.*, vol. 5, pp. 126–129, 1981.

[4] R. Knight, J. Goodling, and D. Hall, "Optimal thermal design of forced convection heat sinks- analytical," *ASME Journal of Electronic Packaging*, vol. 113, pp. 313–321, 1991.

[5] L. Dong and S. Garimella, "Analysis and optimization of the termal performance of microchannel heat sinks," *CTRC Research Publications*, p. Paper 59, 2005.

[6] F. Y. Lim, S. Abdullah, and I. Ahmad, "Numerical study of fluid flow and heat transfer in microchannel heat sinks using anisotropic porous media approximation," *J. of App. Sci.*, vol. 10, no. 18, pp. 2047–2057, 2010.

[7] J. Joseph, R. Nacereddine, M. Delanaye, A. Giraldo, M. Roubah, and J. Brandner in *Proc. of 6th Micro and Nano Flows Conf. 6-7 Sep, Atlanta USA*, Sept. 2018.

[8] J. Joseph, R. Nacereddine, M. Delanaye, J. G. Korvink, and J. J. Brandner, "Advanced numerical methodology to analyze high-temperature wire-net compact heat exchangers for a micro-combined heat and power system application," *Heat Transfer Engineering*, vol. 0, no. 0, pp. 1–13, 2019.

[9] D. Rehman, J. Joseph, G. Morini, M. Delanaye, and J. Brandner in *Proc. of 37th UIT Heat Transfer Conf. 24-26 June,Padova Italy*, 2019.

[10] J. Abraham, E. Sparrow, and J. Tong, "Breakdown of laminar pipe flow into transitional intermittency and subsequent attainment of fully developed intermittent or turbulent flow," *Numerical Heat Transfer, Part B: Fundamentals*, vol. 54, no. 2, pp. 103–115, 2008.

[11] W. Minkowycz, J. Abraham, and E. Sparrow, "Numerical simulation of laminar breakdown and subsequent intermittent and turbulent flow in parallel-plate channels: Effects of inlet velocity profile and turbulence intensity," *International Journal of Heat and Mass Transfer*, vol. 52, no. 17-18, pp. 4040–4046, 2009.

[12] Y. Yang, G. L. Morini, and J. J. Brandner, "Experimental analysis of the influence of wall axial conduction on gas-to-gas micro heat exchanger effectiveness," *Int. J. Heat & Mass Transfer*, vol. 69, pp. 17–25, 2014.

[13] Y. Yang, I. Gerken, J. J. Brandner, and G. L. Morini, "Design and experimental investigation of a gas-to-gas counter-flow micro heat exchanger," *Experimental Heat Transfer*, vol. 27, no. 4, pp. 340–359, 2014.

[14] I. Gerken, J. J. Brandner, and R. Dittmeyer, "Heat transfer enhancement with gas-to-gas micro heat exchangers," *App. Thermal Eng.*, vol. 93, pp. 1410–1416, 2016.

[15] K. Koyama and Y. Asako, "Experimental investigation of heat transfer characteristics on a gas-togas parallel flow microchannel heat exchanger," *The Open Transport Phenomena J.*, vol. 2, no. 3, pp. 1–8, 2010.

[16] K. Koyama and Y. Asako, "Experimental investigation of heat transfer characteristics on a gas-togas counterflow microchannel heat exchanger," *Experimental Heat Transfer*, vol. 23, no. 2, pp. 130–143, 2010.

[17] D. Rehman, G. L. Morini, and C. Hong, "A comparison of data reduction methods for average friction factor calculation of adiabatic gas flows in microchannels," *Micromachines*, vol. 10, no. 3, p. 171, 2019.

[18] C. Hong, G. Tanaka, Y. Asako, and H. Katanoda, "Flow characteristics of gaseous flow through a microtube discharged into the atmosphere," *Int. J. Heat & Mass Transfer*, vol. 121, pp. 187–195, 2018.

[19] Y. Yang, *Experimental and Numerical Analysis of Gas Forced Concection through Microtubes and Micro Heat Exchangers*. PhD dissertation, Alma Mater Studiorum- Universita di Bologna, 2012.

[20] C. Renault, S. Colin, S. Orieux, P. Cognet, and T. Tzédakis, "Optimal design of multi-channel microreactor for uniform residence time distribution," *Microsystem Technologies*, vol. 18, no. 2, pp. 209–223, 2012.